Comparison and Evaluation of Two ABL Mixing Schemes in HWRF

Jian-Wen Bao (NOAA/ESRL/PSD)

Sara A. Michelson (NOAA/ESRL/PSD)

S. G. Gopalakrishnan (NOAA/AOML/HRD)

Frank Marks (NOAA/AOML/HRD)

Jun Zhang (NOAA/AOML/HRD)

Vijay Tallapragada (NOAA/NCEP/EMC)

Presented at
The 66th Interdepartmental Hurricane Conference
Charleston, SC, 5-8 March 2012

Outline

1. **Function of ABL parameterization schemes in NWP models**
2. **Summary of two ABL schemes in the HWRF model**
3. **Comparison in HWRF idealized intensification experiments**
4. **Preliminary conclusions**

What does the ABL parameterization scheme do?

- **Sub-grid turbulence transports temperature, moisture and momentum (+ tracers).**

- **Attempts to integrate effects of sub-grid scale turbulent motion on prognostic variables at grid resolution.**

Operational measure for success: correct model output on the grid-resolved scales everywhere in the model domain.

Scientific measure for success?

Challenge: The simulated turbulent mixing is quite dependent on the definition of the ABL depth and structure!

Two ABL Schemes in the HWRF Model

- The **NMM ABL scheme (MYJ):** *K*-theory, 1.5-oder turbulent kinetic energy (TKE) prognostic equation with non-singular realization

$$\overline{u'w'} = -K_M \frac{\partial u}{\partial z}, \qquad \overline{c'w'} = -K_C \frac{\partial C}{\partial z}$$

$$K_M = P_r^{-1} K_C = \alpha_M \, l_M \sqrt{TKE}$$

- The **GFS ABL scheme:** non-local closure with modifies *K*-profile of Troen and Mahrt (1986)

$$\overline{u'w'} = -K_M \frac{\partial u}{\partial z}, \qquad \overline{c'w'} = -K_C \frac{\partial C}{\partial z} + \overline{c_{nl}'w'}$$

$$K_M = P_r^{-1} K_C = w_s \, \kappa \, h \, (z/h)(1 - z/h)^2$$

where $\overline{c_{nl}'w'}$ is the non-local flux representing the influence of the large-eddy mixing in the ABL with convection.

Property Summary of the Two Schemes

1. The **GFS scheme** assumes that there is a well defined layer *h* in which the vertical distribution of diffusivities follows a special cubic polynomial function $x(1-x)^2$, where x = z/h.

2. The **MYJ scheme** naturally links the ABL depth to the sub-grid TKE distribution, though it does require a specification of the mixing length.

3. The magnitude of the diffusivities from the **GFS scheme** is determined by the ABL depth, while in the **MYJ scheme** it is determined by the mixing length.

Table of Experiments

Experiment Name	ABL Scheme	Surface Layer Scheme	Convective Parameterization Scheme	Profile of Vertical Diffusivity
MYJ/GFS	MYJ	GFS	SAS on both grids	Original
MYJ/GFS/NOCPS	MYJ	GFS	None on both grids	Original
MYJ/GFS/0.9alph	MYJ	GFS	SAS on both grids	Original, Increase ALPH to 0.9
GFS/GFS	GFS	GFS	SAS on both grids	Original
GFS/GFS/NOCPS	GFS	GFS	None on both grids	Original
GFS/GFS/0.5vertdiff8pfac	GFS	GFS	SAS on both grids	0.5 Vertical Diffusion, Increase PFAC to 8
GFS/GFS/0.25vertdiff	GFS	GFS	SAS on both grids	0.25 Vertical Diffusion
GFS/GFS/8PFAC	GFS	GFS	SAS on both grids	Original, Increase PFAC to 8

model grid spacing: dx = dy = ~9 km, ~ 3 km, kx = 43 (NMM sigma-p levels); operational microphysics and radiation schemes

Conventional Intensity Comparisons

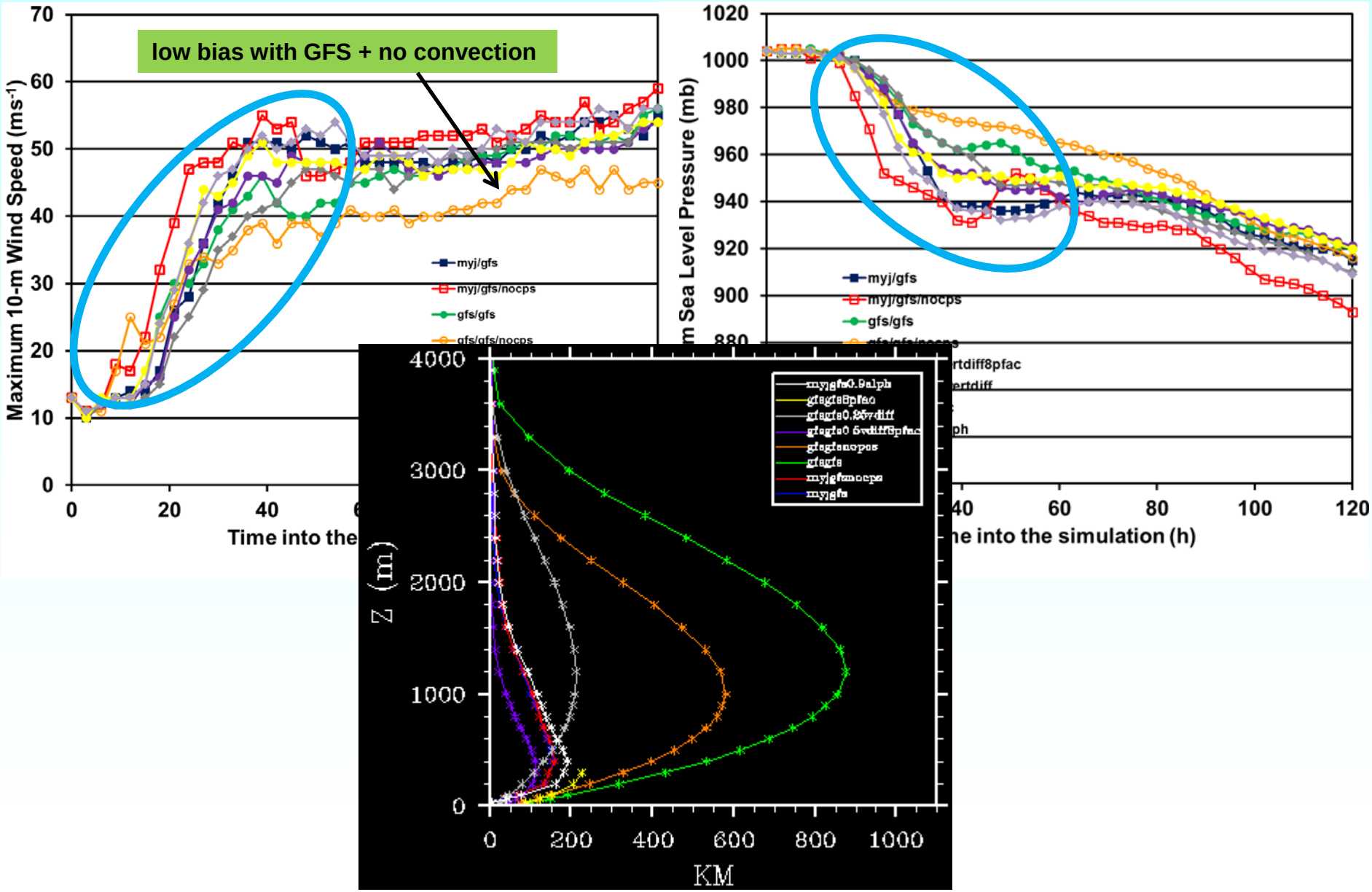

Comparisons of vertical eddy diffusivities with observations at 500 m AMSL

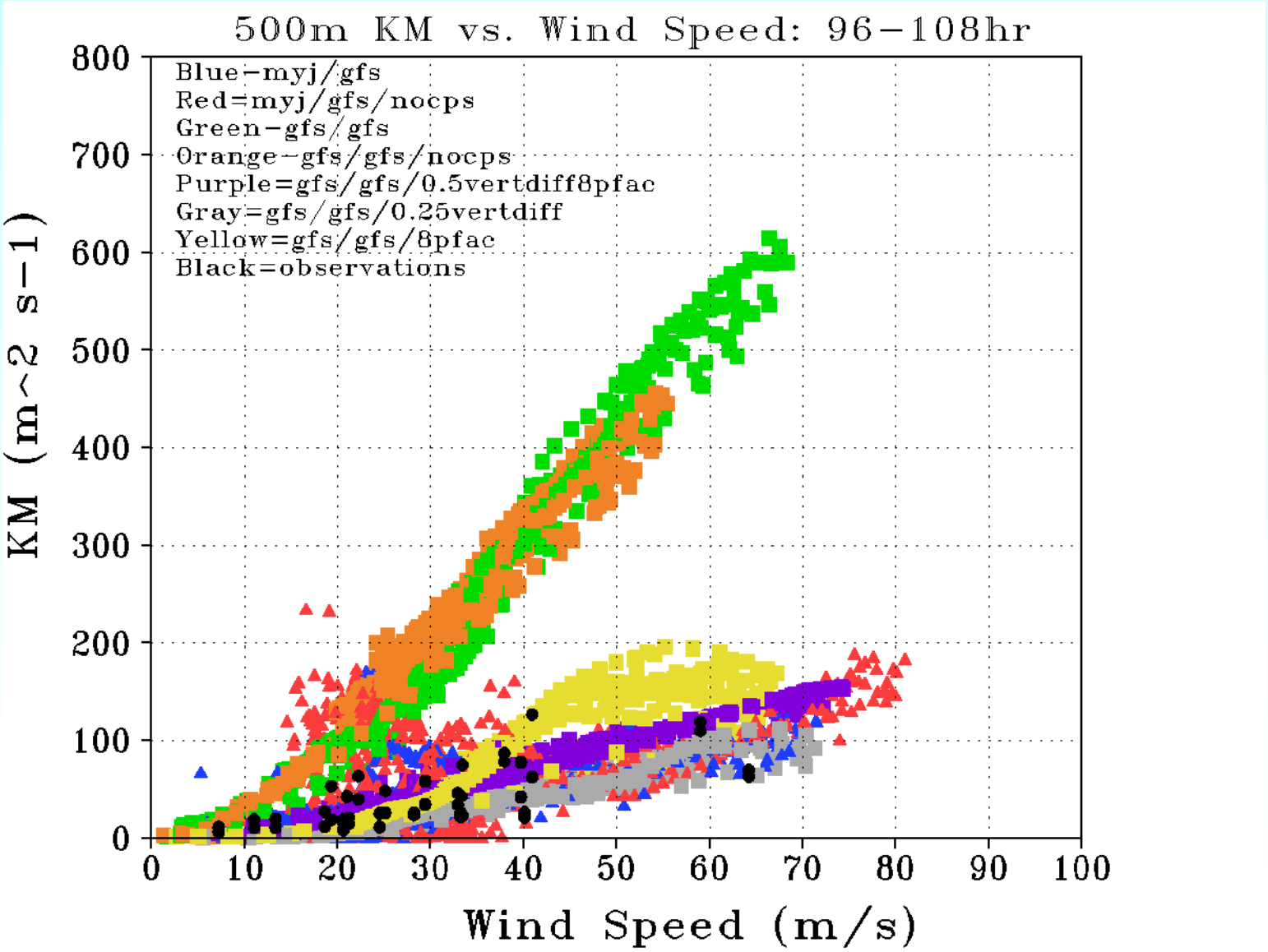

Eddy diffusivity profile and magnitude control the depth of BL inflow and tangential acceleration averaged over 96-108 h: MYJ vs GFS

MYJ GFS

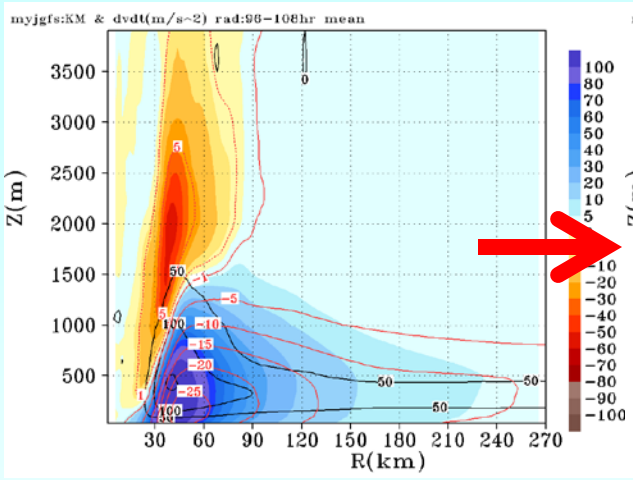

MYJ GFS noCPS

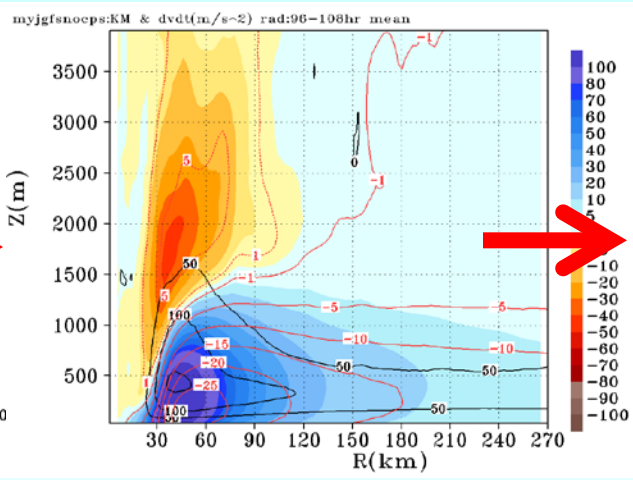

MYJ K_m Profile

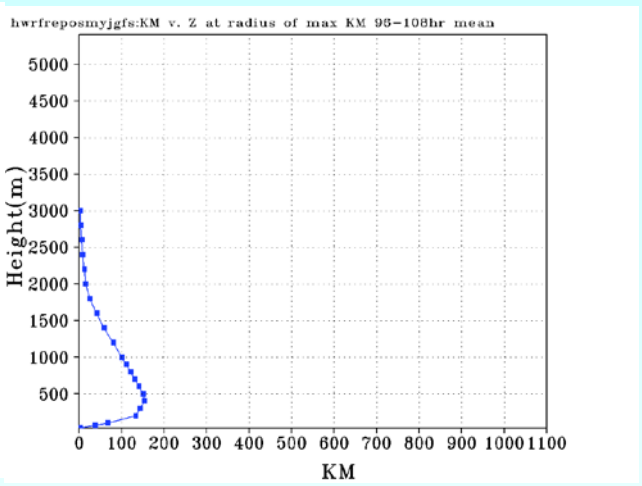

GFS GFS

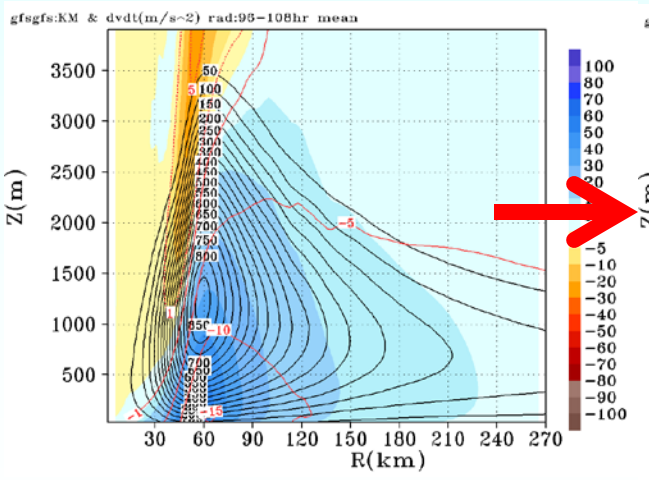

GFS GFS nocps

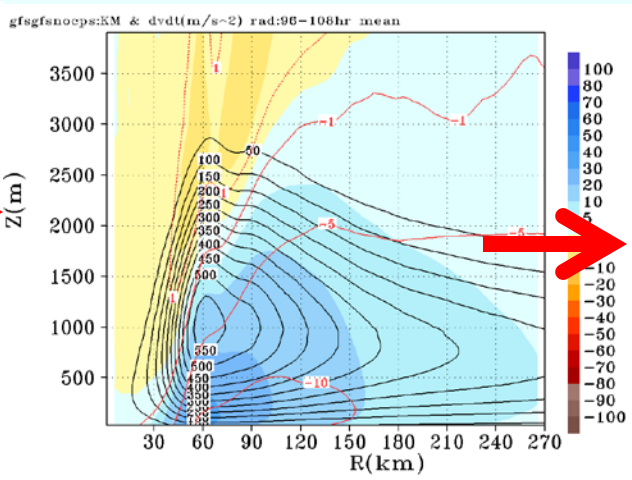

GFS K_m profile

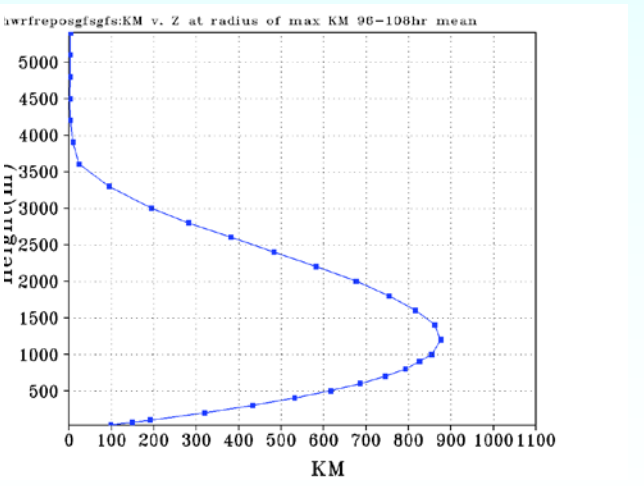

Left 2 rows: Azimuthally averaged tangential acceleration (color shaded, $ms^{-1}h^{-1}$), radial wind speed (red contours, contour interval 5 ms^{-1}) and K_m (black contours, contour interval 50 m^2s^{-1}). Right: K_m profiles

Impact of the magnitude of diffusivity on tangential acceleration and R-Z wind structure averaged over 96-108 h: GFS inter-comparison

GFS 0.25 v-diff

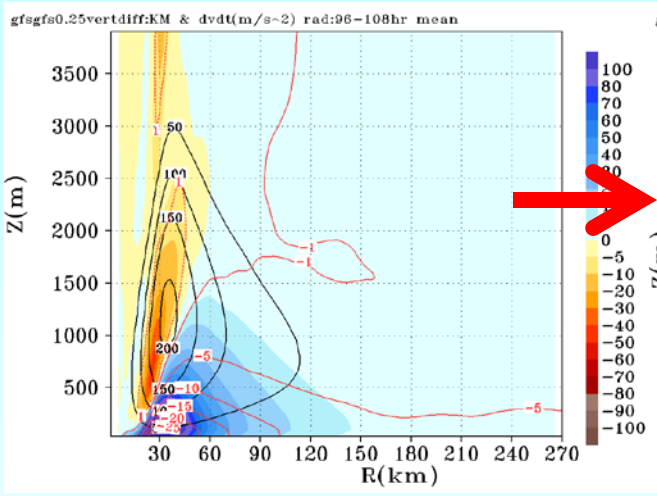

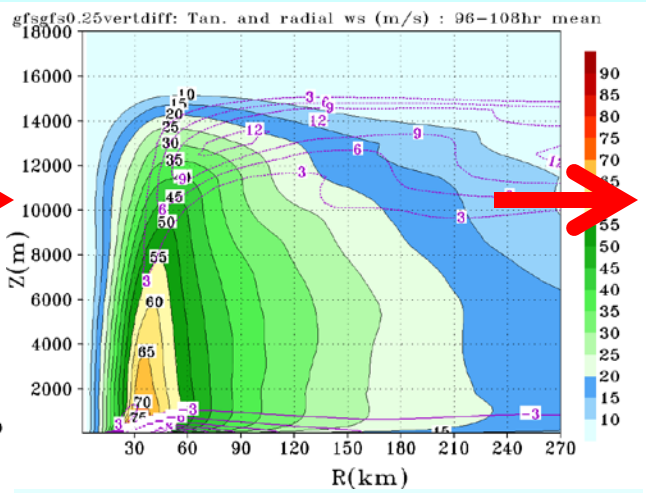

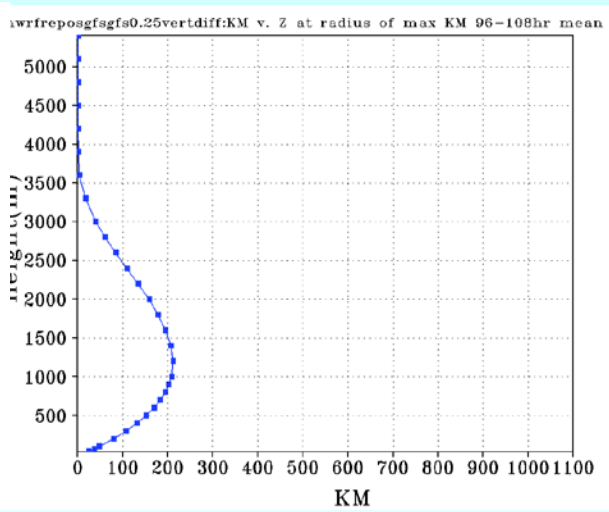

GFS GFS

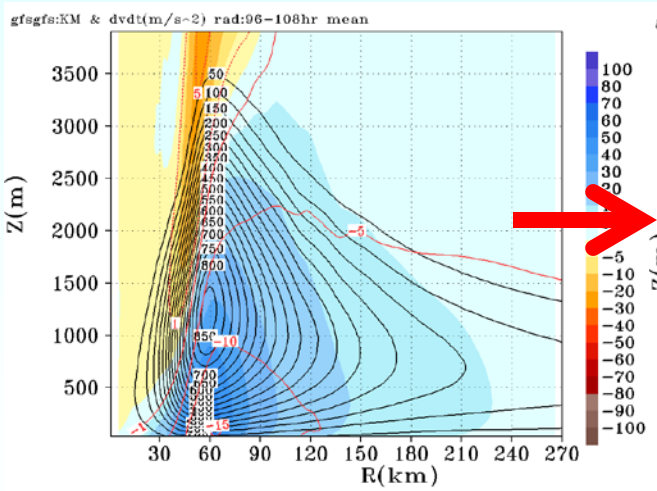

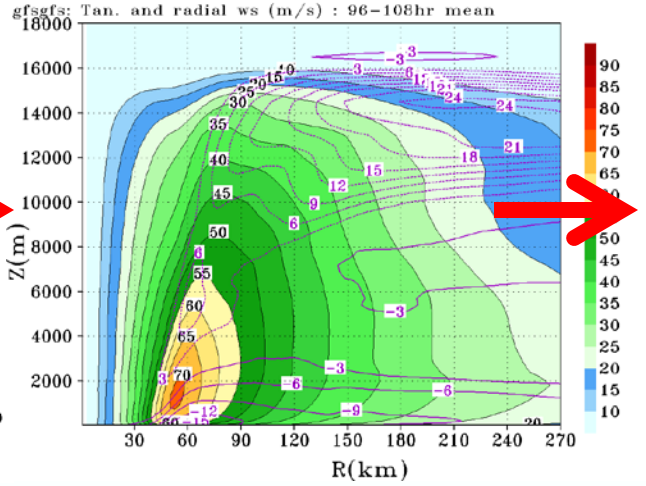

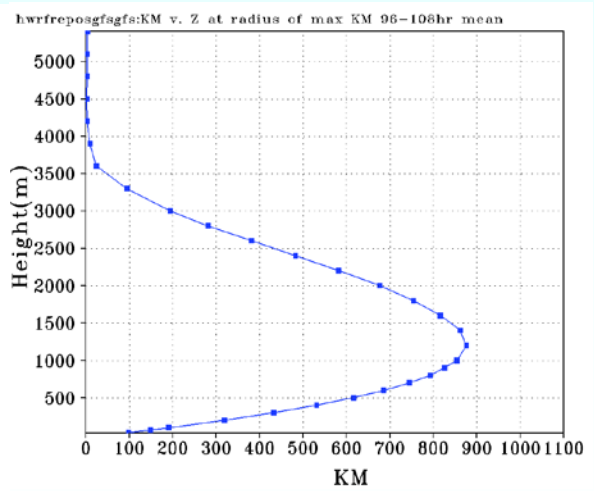

Azimuthally averaged tangential acceleration (color shaded, $ms^{-1}h^{-1}$), radial wind speed (red contours, contour interval 5 ms^{-1}) and K_m (black contours, contour interval 50 m^2s^{-1})

Azimuthally averaged tangential wind speed (color shaded, contour interval 5 ms^{-1}) and radial wind speed (purple contours, contour interval 3 ms^{-1})

K_m Profile

Impact of Zkmax on the depth of BL inflow and tangential acceleration averaged over 96-108 h: GFS inter-comparison

GFS 0.25v diff

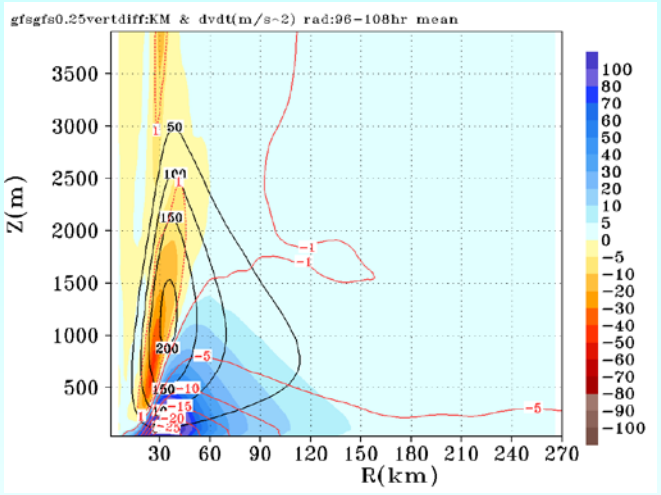

K_m

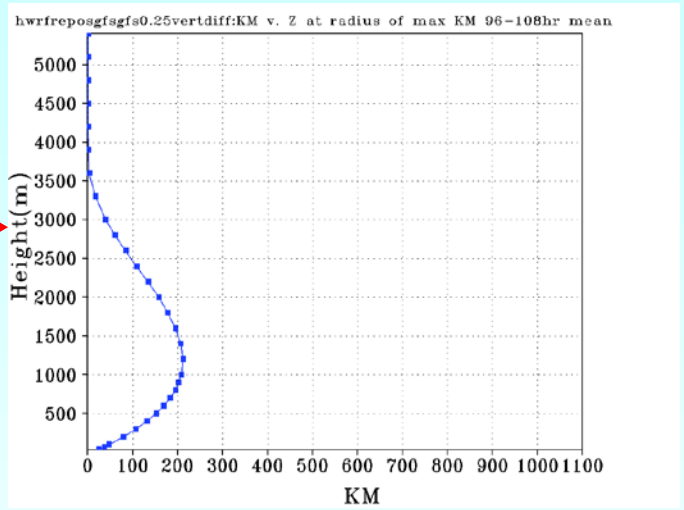

GFS 8pfac

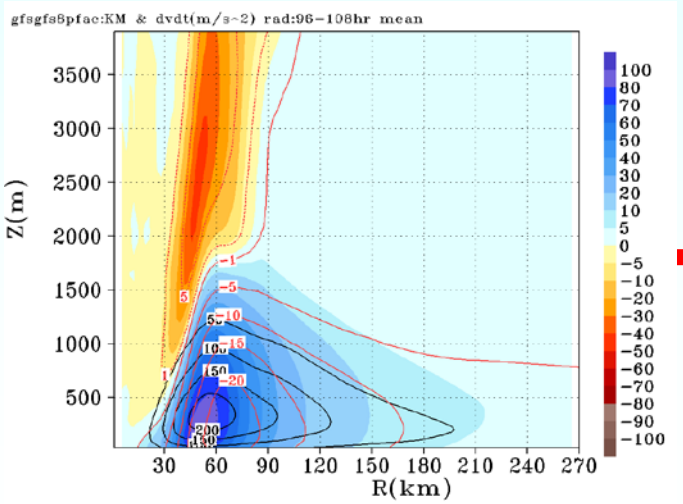

K_m

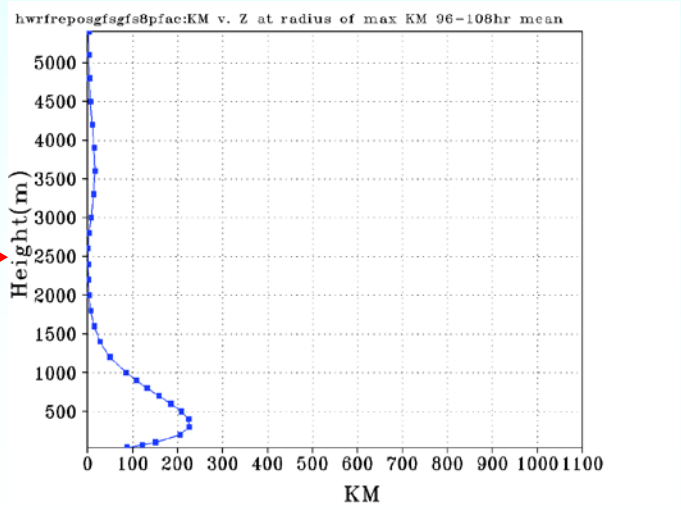

Left: Azimuthally averaged tangential acceleration (color shaded, $ms^{-1}h^{-1}$), radial wind speed (red contours, contour interval 5 ms^{-1}) and K_m (black contours, contour interval 50 m^2s^{-1}). Right: K_m profiles

Impact of the magnitude of diffusivity on the tangential acceleration and the R-Z wind structure averaged over 96-108 h: MYJ inter-comparison

MYJ GFS

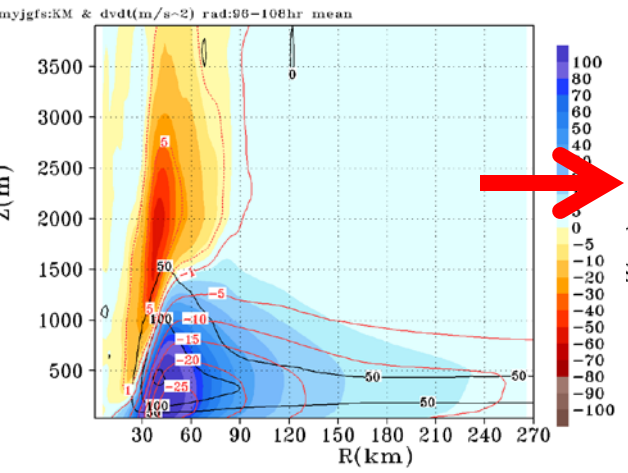

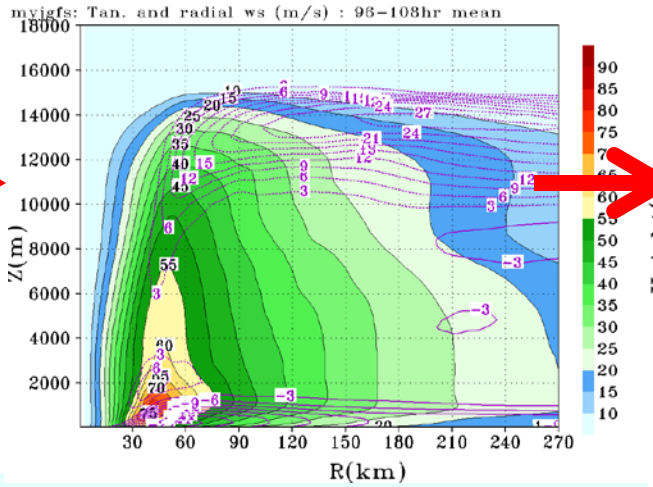

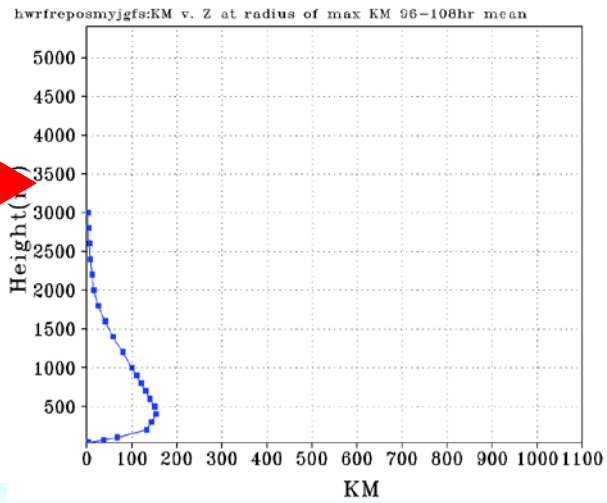

MYJ GFS SFCLAY 0.9 alph

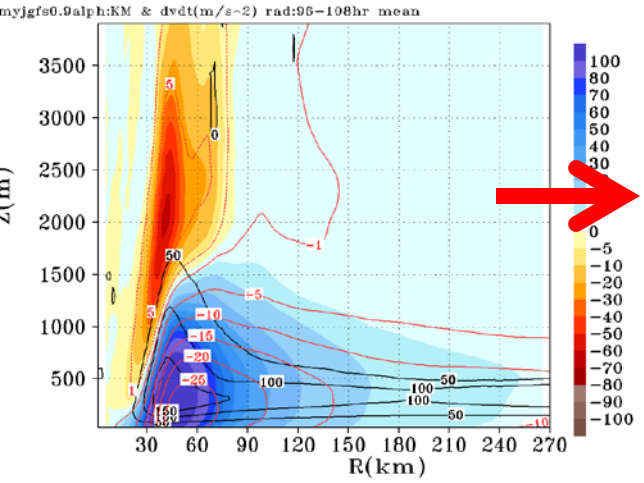

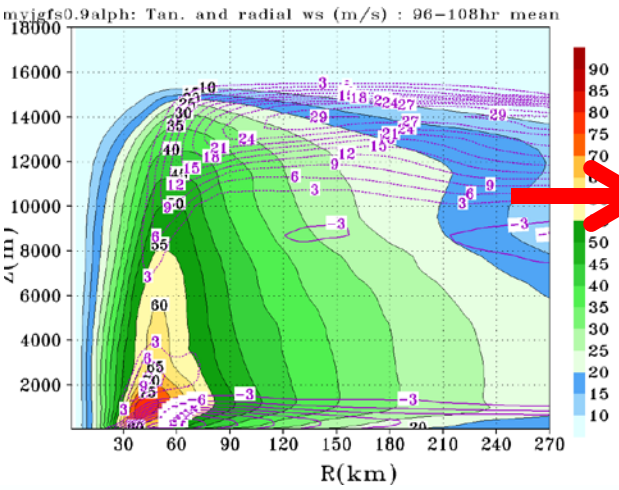

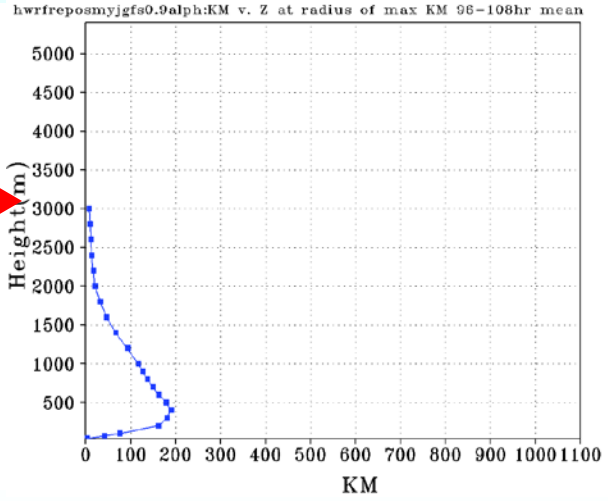

Azimuthally averaged tangential acceleration (color shaded, $ms^{-1}h^{-1}$), radial wind speed (red contours, contour interval 5 ms^{-1}) and K_m (black contours, contour interval 50 m^2s^{-1})

Azimuthally averaged tangential wind speed (color shaded, contour interval 5 ms^{-1}) and radial wind speed (purple contours, contour interval 3 ms^{-1})

K_m Profile

GFS with MYJ-like diffusivity profile vs GFS profile averaged over 96-108 h

MYJ GFS

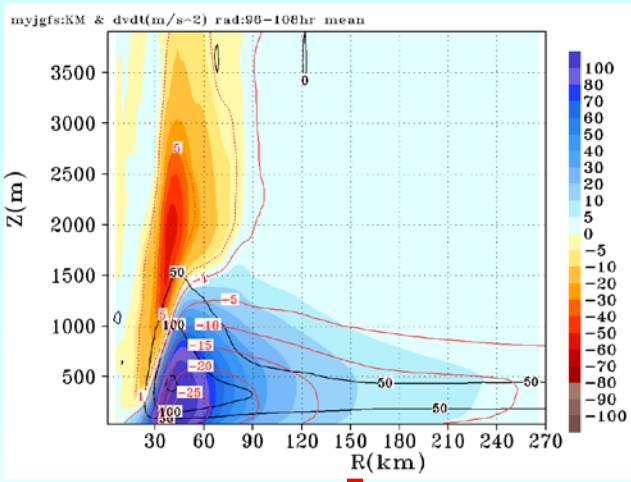

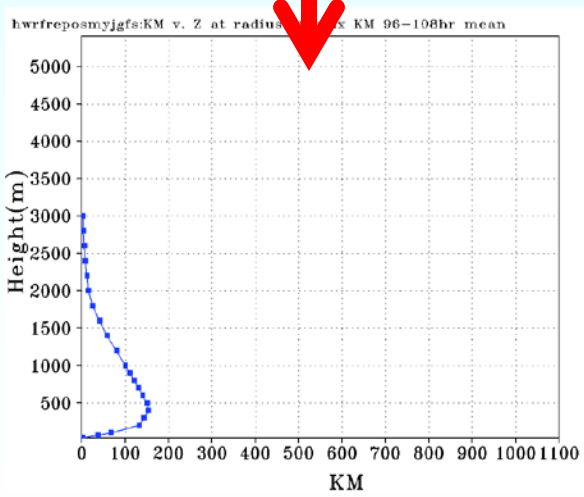

GFS GFS

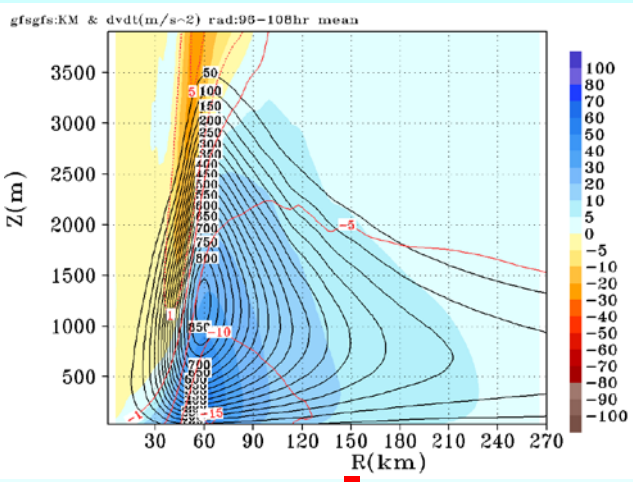

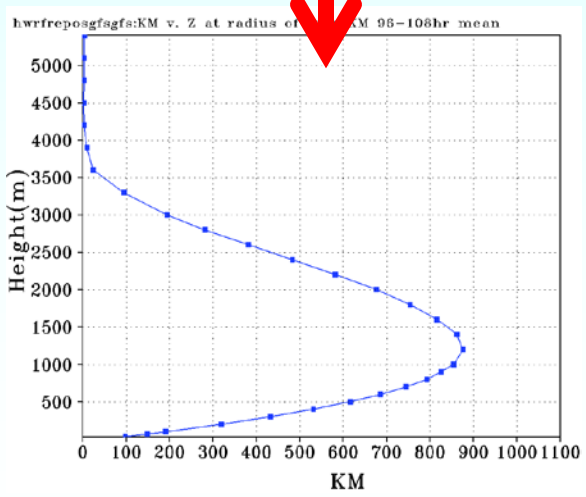

GFS GFS 0.5v diff 8pfac

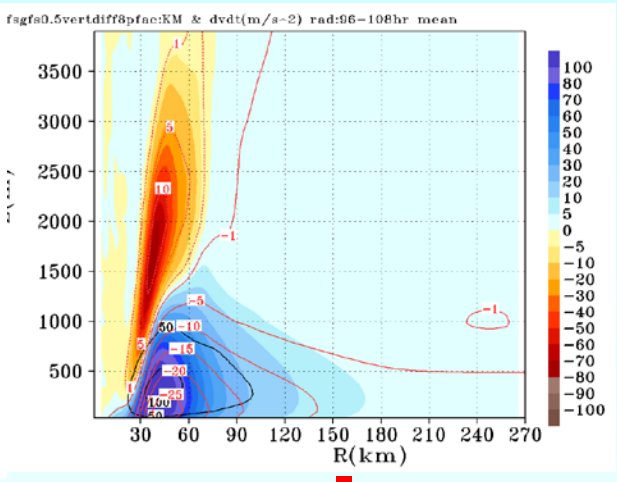

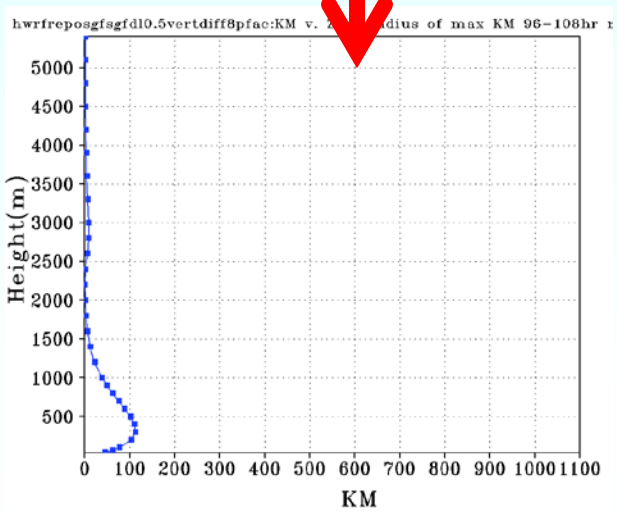

Top: Azimuthally averaged tangential acceleration (color shaded, $ms^{-1}h^{-1}$), radial wind speed (red contours, contour interval 5 ms^{-1}) and K_m (black contours, contour interval 50 m^2s^{-1}). Bottom: K_m profiles

Preliminary Conclusions

1. The intensification rate is influenced by both the profile and magnitude of the vertical eddy diffusivity.

2. Comparisons with limited observations appear to be in favor of the MYJ scheme in terms of the magnitude of diffusivities, but we do not have conclusive results for the vertical profile.

3. The simulated intensification using the GFS scheme is more sensitive to the use of the SAS convection scheme than the MYJ scheme.

4. The R-Z structure of the simulated TC in terms of the enclosed area of 55 m/s becomes broader as the magnitude of the eddy diffusivities increase in both schemes, but the MYJ scheme produces a shallower BL inflow than the GFS scheme.

5. When the GFS scheme is used, the tangential acceleration above the ABL inflow increases as the magnitude of eddy diffusivities decrease, while it is opposite when the MYJ scheme is used.

6. It is possible to change the profile and magnitude of the GFS diffusivities to mimic those of the MYJ scheme.